DIC of plate behaviour under buried blast loading, residual displacement, and correlation with spall pattern

R. Waddoups[1,2,a] , S.D. Clarke[1,2], R.J. Curry[1], T. Lodge[1,2], A. Hibbert[1,2]

[1]University of Sheffield, UK, [2]Blastech Ltd., UK

[a]r.waddoups@sheffield.ac.uk

Abstract. Shallow-buried charges (i.e. landmines) can have destructive effects on people and structures, with work required to capture the distribution of loading on above-ground structures. Deformation of plates under buried charge loading has been recorded during the transient phase using high-speed digital image correlation (DIC) on a reduced area, with full-plate residual deformation also captured via the DIC method. Further, the loading distribution has been captured by determining the spall pattern of paint on the loaded face of the plates.

Introduction

Previous work has found that soil conditions have substantial effects on buried charge loading, both for global impulse measurements and discrete specific impulse measurements [1,2]. It was hypothesised in [3,4] that varying soil type to include coarse particles may result in increased loading from individual particle impacts, which was shown to be the case in [5]. This paper further explores methods of determining the loading distributions in one of these tests.

Methodology

Blast loading. Testing was conducted with 78g PE4 cylindrical charges (57mm diameter, 19mm height) in open-topped 3D-printed cases buried 28mm below the soil surface. A stand-off distance of 140mm from the soil surface to a 4mm thick S275 steel plate was maintained for all tests. The burial medium was varied to establish the effect of particle size in saturated conditions; to establish if larger particles resulted in discrete strikes due to increased individual momentum, rather than a uniform wave of loading. In this paper, data from a single uniform ‘pea’ gravel test is shown.

DIC measurement. Each 450mm square plate, mounted between 20mm thick clamp frames using 12 M12 bolts with an exposed circular area of 315mm diameter, was sand-blasted on one face then painted with a white spray primer. After painting, the back (sand-blasted) face had a 0.10” (2.54mm) speckle pattern applied using black ink and a Correlated Solutions roller. This was applied in four passes at 45 degrees to one another to ensure a consistent pattern was achieved with a sufficient speckle density. The clamp frame was supported by an effectively rigid reaction frame. This arrangement is shown in Figure 1(a) & (c).

The plate was recorded by a pair of Photron FASTCAM SA-Z 2100K high-speed video cameras with a frame rate of 210k frames per second during loading. A resolution of 384 x 160px was achieved over a field of view of approximately 230 x 100mm (~1.6 px/mm) for the transient DIC, with the full plate area captured using full-frame 1024x1024px images before and after testing (enabling residual deformation to be determined). The cameras were positioned with an included angle of approximately 30 degrees, as shown in Figure 1(b). The setup was calibrated with approximately 30 pairs of images using a Correlated Solutions target board.

Figure 1: (a) Clamped plate over soil container, (b) HSV camera setup, (c) Top view of plate after a test

Spall pattern. The front (loaded) face was also painted with white spray primer. This surface was not prepared by sand-blasting, allowing the paint and mill-scale to spall off the plate upon impact.

Results

The transient DIC, processed using Vic-3D, was used to determine plate displacement and velocity, which was in turn used to infer specific impulse as the plate momentum per unit area via Equation 1, a methodology previously used by [6-8]. Distributions of velocity for varying soil types in this series are discussed in [5].

$$v = \frac{i}{\rho t} \quad \text{where } v = \text{velocity, } i = \text{specific impulse, } \rho = \text{plate density, and } t = \text{plate thickness} \qquad (1)$$

Normalised specific impulse. A trend for specific impulse with radius (curve fitting a Gaussian profile to the moving mean of the data) was determined across the test series (for 6 tests involving saturated soils), with the resulting function used to normalise the specific impulse seen at any location on a plate. This resulted in a normalised heatmap of loading across the measured plate area (as shown in Figure 2).

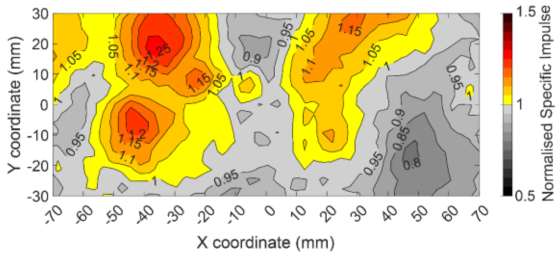

Figure 2: Normalised specific impulse distribution for a uniform ‘pea’ gravel test

Residual deflection. Plate residual deflections were determined from the DIC (Figure 3(a)). A baseline dome profile for each test was extracted from this data using a 2-D convolution method. This profile was then subtracted from the original deformation surface to determine the height of any local peaks (Figure 3(b)).

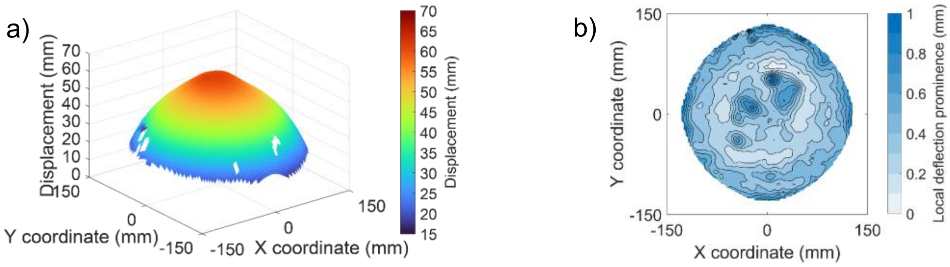

Figure 3: (a) Residual deflection profile as extracted from DIC, (b) global-dome-subtracted residual deflection

Spall pattern correlation. In order to further ascertain the loading distribution on the plate, DSLR images of the spalled paint on the front of the plate (such as in Figure 4(a)) were analysed. In order to process the images a black and white filter was applied, followed by a brightness threshold filter. This allowed for a qualitative inspection of strike locations, as in Figure 4(b), which can be seen to correlate with locations of increased specific impulse and residual deflection in Figure 4(c).

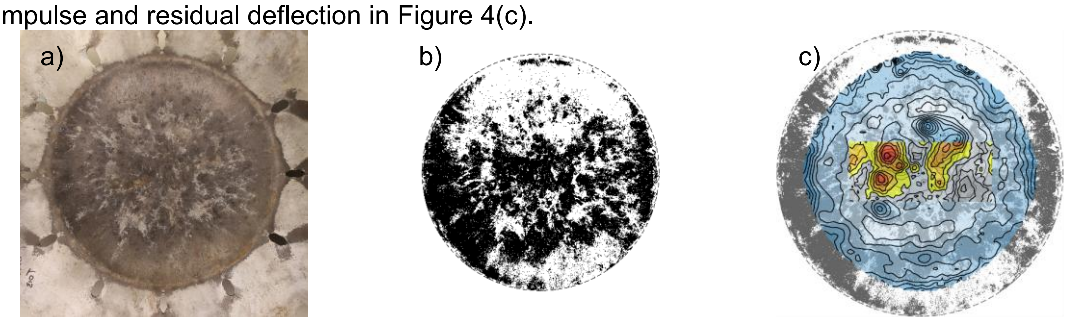

Figure 4: (a) Image of front face of plate after testing, (b) threshold-filtered spall pattern,
(c) layered specific impulse map, global-dome-subtracted residual deflection and spall pattern

Conclusion

High-speed DIC, static DIC, and paint spalling have each been used to characterise the loading distribution from a buried explosive charge. Localised regions of increased loading have been identified, which can be seen to correlate with increased residual deflection and paint spall. This work demonstrates that methodologies with varying levels of complexity can be used to cross-validate within a single blast loading experiment.

References

[1] Clarke, S. D., Fay, S. D., Warren, J. A., Tyas, A., Rigby, S. E., Reay, J. J., Livesey, R., & Elgy, I. (2017). Predicting the role of geotechnical parameters on the output from shallow buried explosives. International Journal of Impact Engineering, 102, 117–128. https://doi.org/10.1016/j.ijimpeng.2016.12.006

[2] Clarke, S., Rigby, S., Fay, S., Barr, A., Tyas, A., Gant, M., & Elgy, I. (2020). Characterisation of buried blast loading. Proceedings of the Royal Society A: Mathematical, Physical and Engineering Sciences, 476(2236). https://doi.org/10.1098/rspa.2019.0791

[3] Rigby, S. E., Fay, S. D., Tyas, A., Clarke, S. D., Reay, J. J., Warren, J. A., Gant, M., & Elgy, I. (2018). Influence of particle size distribution on the blast pressure profile from explosives buried in saturated soils. Shock Waves, 28(3), 613–626. https://doi.org/10.1007/s00193-017-0727-7

[4] Waddoups, R., Clarke, S., Tyas, A., Rigby, S., Gant, M., & Elgy, I. (2023). An Approach to Quantifying the Influence of Particle Size Distribution on Buried Blast Loading. Eng, 4(1), 319–340. https://doi.org/10.3390/eng4010020

[5] Waddoups, R., Clarke, S. D., Curry, R. J., Lodge, T. J., & Hibbert, A. (2026). DIC determination of localised loading on blast loaded plates from coarse soils. *Submitted to:* Light-Weight Armour for Defence & Security LWAG 2026.

[6] Tetlow, L., Rigby, S. E., Langdon, G. S., Curry, R. J., & Pezzola, G. (2026). Experimental characterisation of near-field blast loading using digital image correlation on thin plates. International Journal of Impact Engineering, 213. https://doi.org/10.1016/j.ijimpeng.2026.105671

[7] Curry, R. J., Langdon, G. S., & Tyas, A. (2025). Steel Plates Subjected to Localised Blast Loading: Transient Measurements Using Ultra-High-Speed Camera Technology. Strain, 61(6). https://doi.org/10.1111/str.70019

[8] Rigby, S. E., Tyas, A., Curry, R. J., & Langdon, G. S. (2019). Experimental Measurement of Specific Impulse Distribution and Transient Deformation of Plates Subjected to Near-Field Explosive Blasts. Experimental Mechanics, 59(2), 163–178. https://doi.org/10.1007/s11340-018-00438-3